Biochimica et Biophysica Acta, 557 (1979) 62—78

BBA 78524

THE INTERACTION OF VARIOUS LANTHANIDE IONS AND SOME ANIONS WITH PHOSPHATIDYLCHOLINE VESICLE MEBRANES

A ^{31}P NMR STUDY OF THE SURFACE POTENTIAL EFFECTS

JAN WESTMAN and L.E. GÖRAN ERIKSSON

Department of Biophysics, University of Stockholm, Arrhenius Laboratory, S-106 91 Stockholm (Sweden)

(Received March 22nd, 1979)

Key words: Phosphatidylcholine; Ion effect; ^{31}P-NMR; Surface potential; Lanthanide; (Membrane vesicle)

Summary

The interaction of various lanthanide ions with vesicles of phosphatidylcholine from egg yolk has been followed by ^{31}P NMR at 30°C. From known magnetic properties of these ions, separation of the paramagnetic shift into a pure contact and a pseudo-contact part was carried out. Binding curves for the contact contribution (F curves) were obtained from vesicles in solutions of sodium salts with monovalent anions over a wide concentration range. These curves should be insensitive to any conformational effects due to ion binding. Indication of a conformational change in the lipid head group at low ion binding was obtained by studying the ratio between the contact and the pseudo-contact contributions. Besides the adsorption of lanthanide ions, specific anion binding to the surface was introduced to account for the enhanced chemical shifts ($Cl^- < Br^- < NO_3^-$). The results were analyzed in terms of the theory for the diffuse double layer (Gouy-Chapman-Grahame) with equilibrium conditions for the adsorbing cations and anions. Simulations of the titration curves furnished parameters for the ion-lipid interactions. The synergism between the cations and anions follows from the potential effects. Comparison of results with lanthanide ions and Ca^{2+} indicates that the anion adsorption probably depends on the nature of the adsorbed cation. Lanthanide ion binding to L-glycerophosphorylcholine is not influenced by sodium salts. The binding constant for this complex is weaker than with phosphatidylcholine. The chemical shifts for the lanthanide ion complexes with these two phosphorus compounds seem to be about the same.

Introduction

Phosphatidylcholine constitutes the major lipid material in many biological membranes. Although this lipid is an electrically neutral zwitterion at physiological pH values it can bind di- and trivalent cations at the membrane surface. In this context Ca^{2+} is of importance due to its many physiological functions. However, Ln^{3+} often mimics the properties of Ca^{2+} and therefore competes with the latter in biological systems. The coordination geometry of Ca^{2+} and Ln^{3+} are probably different, but Ln^{3+} as a probe will still reflect the general scheme for the adsorption of cations to the membrane surface. Since the coordination takes place at the phosphorus sites ^{31}P NMR is useful as we have shown [1]. Interaction with Ca^{2+} induces weak but measurable chemical shifts due to the metal binding to phosphatidylcholine vesicles [1,2]. Several Ln^{3+} have paramagnetic properties making them suitable to study the ion-lipid interaction. Numerous papers have appeared where phosphatidylcholine vesicles in the presence of Ln^{3+} have been studied by means of NMR for various nuclei [1–5]. We have recently published a ^{31}P NMR study of Ln^{3+} binding to vesicles of phosphatidylcholine from egg yolk at different ionic strength produced with NaCl [1]. The equilibria behind the adsorption were investigated, and we stressed the importance of the surface potential effects. These were analyzed in terms of the theory for the diffuse double layer (Gouy-Chapman) making it possible to derive intrinsic binding constants. McLaughlin et al. [5] have studied Co^{2+} as a divalent paramagnetic probe with ^{31}P NMR. However, since its binding constant is as low as for Ca^{2+}, high concentrations of this ion are required in order to get measurable effects. The results from Co^{2+} experiments were analyzed by them in a manner similar to the approach employed by us for Ca^{2+} and Ln^{3+}. An interesting confirmation of the surface potential effects were obtained by McLaughlin et al. with an independent determination of ζ-potentials with electrophoresis. The Gouy-Chapman theory has been applied by Puskin [6] in an EPR study of Mn^{2+} binding to various phospholipids and by Nir et al. [7] in their equilibrium dialysis experiments on Mg^{2+} and Ca^{2+} with phosphatidylserine.

In our preceding work [1] we noticed some discrepancies between the results obtained for the initial range of the titration curves and those based on a curve-fitting procedure more strongly emphasizing the subsequent part. No detailed analysis of this observation was attempted at that time. One obvious possibility would be some structural rearrangement taking place in the surface due to ion interactions.

Recently some NMR evidence for a conformational change due to lanthanide binding has been presented [8,9]. However, according to Barsukov et al. [10] the conformation is independent of the presence of lanthanide ions. Also the average motional rate of phosphate region should be unaffected by ions [2]. Earlier we used Tb^{3+} as a shift ion because of its large shifts. Structural changes in the surface may, however, influence the ratio between contact and pseudo-contact shifts due to altered intra- as well as intermolecular vectors. In the present work we have therefore extended our previous study using several different lanthanides (La^{3+}, Ce^{3+}, Pr^{3+}, Eu^{3+}, Tb^{3+}) in order to distinguish between contact and pseudo-contact effects. Since the contact contribution to

the shift is isotropic and requires a direct overlap between the metal orbitals and those of the phosphorus site one expects this type of shift to exhibit minimum sensitivity to conformational effects. From theoretical values [11,12] separation of the shifts into pure contact and pseudo-contact parts have been attempted. Using information from all the ions studied we have derived experimental titration curves for the contact contribution. These so-called *F* curves should more correctly than previous data reflect the formation of lipid-ion complexes.

In order to further test the theory for the diffuse double layer (Gouy-Chapman) we have employed different total electrolyte concentrations (0—1 M) by exposing the vesicles to sodium salts with various monovalent anions (Cl^-, Br^-, NO_3^-). As reported by Hauser et al. [3,4] the ^{31}P NMR shifts were enhanced by anions in the order $Cl^- < Br^- < NO_3^-$. We accounted for this by assuming specific interactions of the anions with the membrane surface [1]. Independently Barsukov et al. [13] have proposed a specific anion adsorption based on their NMR and electrophoresis experiments. The specific anion binding to phosphatidylcholine has recently been questioned by McLaughlin et al. [5]. Contrary to Barsukov et al., they claim that anions (chloride) do not influence the electrophoretic properties of the liposomes. The enhanced lanthanide shift caused by the anions is now further elucidated. We demonstrate an intimate synergism between the cation and anion bindings promoted by the surface potential effect.

To get further information about the intrinsic binding constant for the phosphate-Ln^{3+} interaction we have also studied glycerophosphorylcholine and found its binding to Eu^{3+} to be fairly weak. As expected, in the latter case no sensitivity to ionic strength is found since surface potential effects are not involved.

The improved technique and the large number of experiments now carried out give us confidence to revise the earlier presented binding parameters in order to get a better quantitative agreement with the total material. The main message delivered in our first paper still remains and is emphasized, namely the importance of accounting for the surface potential effects.

Materials and Methods

The experiments with egg yolk phosphatidylcholine vesicles were carried out essentially as described elsewhere [1], but with a more refined control and standardization of the preparations. Since no buffers were employed particular attention was paid to the pH value, which was adjusted to a meter reading of about 3.9 (corresponding to p^2H about 4.3). Also all salt solutions added had pH values close to this figure, and after completing a titration the pH was checked and found never to deviate significantly from the starting value. All samples were analyzed for phosphorus by the standard method of Fiske and Subbarow [14]. The average vesicle size was determined by ^{31}P NMR, without proton decoupling in order not to introduce any errors due to the NOE effect. No systematic and significant variation in vesicle size between the various preparations was observed. Hence, we estimated the outer surface of all the vesicles studied to contain about 65% of the total phosphatidylcholine mole-

cules, a figure used to calculate the total concentration of active phosphorus sites, $[P]_0$. All NMR measurements were made at 30 ± 1°C.

The procedure for titration at high ionic strengths (NaCl, NaBr and $NaNO_3$; 0.1—1.0 M in deuterium oxide) was to add small volumes of a concentrated solution of lanthanide salts to vesicles directly into the NMR tube (10 or 12 mm). The chloride salt of the lanthanides was always used even in the presence of the other anions. $LaCl_3$ (Kebo AB, Sweden), $CeCl_3$, $EuCl_3 \cdot 6H_2O$, $PrCl_3 \cdot 6H_2O$ (Alpha Products, U.S.A.) and $TbCl_3$ (Koch-Light Labs. Ltd., U.K.) were all 99.9% and used without analysis. For the comparison between the set of Ln^{3+} and the construction of the so-called F curves we always carried out all the separate titrations with one single-vesicle stock solution. The different Ln^{3+} salts were added so that the concentrations of the various Ln^{3+} coincided. The shifts were corrected for the small diamagnetic contribution derived from the La^{3+} titrations. For experiments at low and/or constant ionic strength vesicles in salt-free solutions were instead added to the appropriate weak Ln^{3+} solution. In this particular case solutions of $EuCl_3$ and $Eu(NO_3)_3$ were used. The initial slope experiments were performed as described before [1], but now with Eu^{3+} instead of Tb^{3+} and in the presence of 0.1 M NaCl, NaBr or $NaNO_3$.

The experiments with L-α-glycerophosphorylcholine in 0.1 M NaCl at pH about 4 were made with Eu^{3+}, for the complete titration, as well as the other Ln^{3+}, at one single concentration. The initial slope study was done with Eu^{3+} over a wide concentration range of glycerophosphorylcholine (2.4—158 mM). This compound in the form of the cadmium chloride complex (Sigma Chem. Co., grade I) was beforehand converted into the free zwitterionic form by adding Chelex-100 (sodium form) followed by filtration. The pH was lowered to about 4 by HCl and the concentration determined by phosphorus analysis [14].

Two control experiments were performed to see if adsorption of Eu^{3+} to the walls of the NMR tubes took place. In one experiment, some NMR tubes were coated with a hydrophobic coating (Dricote, Fischer Scientific Co.) on the inside and some were uncoated. The shifts obtained at very low $[M]_0/[P]_0$ ratios of low $[P]_0$ values (7.5 mM) did not differ significantly for the two types of tubes. In another experiment the concentrations of Eu^{3+} in a solution were measured colorimetrically by the alizarinsulfonate method [15] before and after the solutions had been shaken several times in NMR tubes. However, no adsorption could be detected.

The simulations were carried out on a DEC 10 system. A standard subroutine NS01A from the Harwell Subroutine Library [16] was used to obtain a full solution of the system of non-linear equations.

Theory

Separation of lanthanide shifts into contact and pseudo-contact parts

The total chemical shift induced by a Ln^{3+} (j) for the ^{31}P nucleus studied can be expressed as

$$\delta_j^{tot} = \delta_j^{dia} + \delta_j^{para} \quad (1)$$

The diamagnetic part is assumed to be equivalent to the shift recorded for La^{3+}. The paramagnetic part is defined as being positive for upfield values (ppm). Separation of the paramagnetic contribution into one term due to contact and another due to pseudo-contact effects has been examined before for various lanthanides [11,12]. At constant temperature and a given crystal-field splitting for an axially symmetric complex, one expects

$$\delta_j^{para} = F \cdot \langle S_z \rangle_j + G \cdot C_j^D \quad (2)$$

The first term accounts for the contact and the second for the pseudo-contact contribution. The factors F and G depend on the nucleus studied (^{31}P), but not on the Ln^{3+} employed. G is a function of the geometry of the actual complex. $\langle S_z \rangle_j$ and C_j^D are theoretically calculated atomic constants (Table I) for each individual Ln^{3+} (j). The ions selected here belong to the first part of the lanthanide group, but cover a contact to pseudo-contact ratio, $\langle S_z \rangle_j / C_j^D$, over a wide range. As seen, Eu^{3+} is the ion of choice when predominantly contact shifts are wanted.

Eqn. 2 gives the paramagnetic shift for the ^{31}P nucleus in a complex with Ln^{3+}. In the case of a fast exchange between complexed and free forms the paramagnetic shift, $\delta_j^{para}(obs)$, will become proportional to the fraction (y) of complexed nuclei, since it is assumed that the free nuclei do not experience any shift. From $\delta_j^{para}(obs) = y \cdot \delta_j^{para}$ and Eqn. 2 we obtain

$$\delta_j^{para}(obs)/C_j^D = y \cdot F \cdot \frac{\langle S_z \rangle_j}{C_j^D} + y \cdot G \quad (3)$$

This equation shows that it should be possible to distinguish the contact and the pseudo-contact parts by employing a set of several Ln^{3+} with different $\langle S_z \rangle_j / C_j^D$ ratios [11,12]. If the basic assumptions behind Eqn. 2 are fulfilled and if the selected Ln^{3+} have very similar physicochemical properties (i.e. complex constants, activity coefficients, etc.) we expect a straight line by plotting $\delta_j^{para}(obs)/C_j^D$ versus the parameter ratio $\langle S_z \rangle_j / C_j^D$. By Eqn. 3 the factor $y \cdot F$ may be obtained from the slope and $y \cdot G$ from the intercept at a fixed y value for all the actual Ln^{3+}. Since this procedure is very demanding we were restricted to use only a few Ln^{3+}, mainly La^{3+}, Ce^{3+}, Eu^{3+} and Tb^{3+}.

We assume that $F(obs)$ will be insensitive to any conformational changes due to the complex formation taking place. The so-called F curves, i.e. F(obs) versus the ratio between the total lanthanide-to-ligand concentrations ($[M]_0$/

TABLE I

THEORETICAL PARAMETERS USED IN EQN. 3 TO SEPARATE THE LANTHANIDE-INDUCED SHIFT INTO CONTACT AND PSEUDO-CONTACT PARTS

Adopted from Refs. 11 and 12.

	$\langle S_z \rangle_j$	C_j^D	$\langle S_z \rangle_j / C_j^D$
Ce	0.970	−6.25	−0.155
Pr	2.972	−10.99	−0.270
Eu	−10.682	4.05	−2.638
Tb	−31.818	−85.26	0.373

$[P]_0$) should faithfully reflect the real binding curve. For the pseudo-contact part we would expect the factor G to vary if there is a conformational change, due to intra- as well as intermolecular effects. The G factor will then be a function of the fraction of complex formation, $G(\text{obs}) = y \cdot G(y)$. As long as no variation in $G(y)$ takes place the ratio of $F(\text{obs})/G(\text{obs})$ should remain constant.

Interaction of cations and anions with the membrane surface

We here extend our published treatment [1] of the surface phenomena in terms of specific binding and the diffuse double layer theory. Only a brief account will be given in the following as the main points are already outlined in our work [1]. As before, we assume the anion X^- (Cl^-, Br^- and NO_3^-) as well as the metal ion M^{3+} to bind to the phospholipids in the surface (s). Thus

$$M^{3+}\,(s) + n\,P \rightleftharpoons MP_n^{3+} \qquad (M^{3+} = Ln^{3+})$$

$$X^-\,(s) + P \rightleftharpoons XP^-$$

where P symbolizes the zwitterionic site and n is the stoichiometry for the metal ion complex. We anticipate that the Ln^{3+} and the anions can bind to all the outer phosphatidylcholine molecules except those already occupied by a cation, respectively an anion. We also include the complex formation between metal ion and anion in the bulk solution (b)

$$M^{3+}\,(b) + X^-\,(b) \rightleftharpoons MX^{2+}\,(b)$$

Absorption of MX^{2+} to the surface is neglected (see Discussion).

As we have shown earlier [1] the relevant equilibrium relations then involve the bulk (b), interface (I), and surface (s) concentrations, giving:

$$K_{MX} = \frac{\gamma_{MX}[MX]_b}{\gamma_M[M]_b\gamma_X[X]_b} \text{ (l/mol)} \tag{4}$$

$$K_X = \frac{[XP]_s}{\gamma_X[X]_I[P]_s} \text{ (l/mol)} \tag{5}$$

$$K_n = \frac{[MP_n]_s}{\gamma_M[M]_I[P]_s^n} \quad ((\text{Å}^2)^{n-1} \cdot \text{l/mol}^n) \tag{6}$$

Values on the constants K_{MX} are found in the literature [17—19]. The appropriate activity factors are assumed to be equal to the bulk values and are denoted by γ [20—23].

The relationships between interface concentrations and bulk concentrations are given by the Boltzmann relation. The Grahame equation gives the relations between the charge on the surface created by the ions bound, the surface potential and the ionic composition in the bulk solution.

$$\sigma = \pm\left(2\,\epsilon\epsilon_0 RT \sum_i [i]_b \left(\exp\left(-\frac{z_i F\psi}{RT}\right) - 1\right)\right)^{1/2} \tag{7}$$

where σ is the surface charge in electronic charges/Å^2, $[i]_b$ is the bulk concentration of the i'th ionic species in mol/l, z_i is its charge, ψ is the surface potential in mV, $F/RT = 26.1$ mV and $(2\epsilon\epsilon_0 RT)^{-1/2} = 274.0$ at 30°C.

The surface charge is created by the bound species.

$$\sigma = \frac{3}{70} \cdot \frac{[MP_n]_s}{[P]_{os}} - \frac{1}{70} \cdot \frac{[XP]_s}{[P]_{os}} \tag{8}$$

The bulk concentrations are calculated as the difference between the total amount of ions added and the amount of ions bound.

Relations between bulk concentrations and surface concentrations are given by $s \cdot [P]_{os} = v \cdot [P]_o$, where v is the total solution volume, s is the total area on the outside of the vesicles, $[P]_o$ is the concentration of phospholipids on the outside of the vesicles in mol/l and $[P]_{os}$ is the external surface concentration (mol/Å^2) of phospholipids. For egg yolk phosphatidylcholine the molecular cross-sectional area at the surface is assumed to be 70 Å^2 even in the presence of Ln^{3+}. This corresponds to $[P]_{os} = 1/70\,N$mol/Å^2. From the experiments we have be means of Eqn. 3 deduced values for

$$F(\text{obs}) = y \cdot F = n \cdot \frac{[MP_n]_s}{[P]_{os}} \cdot F \tag{9}$$

The factor F is now the relevant shift parameter rather than the bound shift used in our earlier work [1].

We thus have a system of non-linear equations with two unknowns $[MP_n]_s/[P]_{os}$ and $[XP]_s/[P]_{os}$ and four input parameters n, F, K_n and K_x. First we find an approximate solution by neglecting the amount of anions bound, compared to those in the bulk solution, and by solving the equations so obtained using Newton's method. The full solution is then calculated by using a library subroutine [16] with the approximate values on $[MP_n]_s/[P]_{os}$ and $[XP]_s/[P]_{os}$ as input values. The constant K_n was introduced in Eqn. 6 as a mixed constant but it is more practical to transform this into $K_n^* = K_n \cdot [P]_{os}^{n-1}$ [1]. This constant then has the dimension of l/mol.

We have also applied the initial slope approach [1] which is valid far from saturation:

$$k = -\frac{\exp(3F\psi/RT)}{\gamma \cdot K_n^*} \cdot \frac{k}{[P]_o} + n \cdot \delta_j^{para} \tag{10}$$

where δ_j^{para} now takes the place of Δ_n used in our earlier work [1]. Here $k = \partial(\delta_j^{para}(\text{obs}))/\partial([M]_o/[P]_o)$ is the initial slope of the titration curve. If the titration is carried out with Ln^{3+} which predominantly gives a contact shift (cf. Eqn. 2), such as Eu^{3+}, it should be possible to directly obtain an estimated value of F from the intercept, $n \cdot \delta_j^{para}$, of the initial slope graph. Hence, this intercept will correspond to $n \cdot F \cdot \langle S_z \rangle_j$ and we have a way to estimate the value of $n \cdot F$. Because of the influence of the anion binding on the surface potential ψ in Eqn. 10 it is not possible to extract K_n^* from the slope of the line. The initial slope lines have to be simulated.

Since the concentration $[P]_o$ was varied between 2.6 and 43.9 mM we have to correct the total solution volume for the space occupied by the vesicles to obtain the effective bulk volume, used to calculate the effective bulk concentrations of the ions. This was taken care of in the simulations.

Results

The separation of the Ln^{3+} shifts into contact and pseudo-contact parts required a careful elimination of systematic errors. In Fig. 1 a plot according to Eqn. 3 is demonstrated for titrations with various Ln^{3+} in the presence of 0.5 M NaCl. The lines are fitted to the values for Ln^{3+} titrated to an identical concentration ratio, i.e. $[M]_o/[P]_o$. As seen, the agreement with straight lines is satisfactory (correlation coefficients around 0.999). Hence, the basic assumptions behind Eqn. 3 seem to be valid and we may proceed to determine $y \cdot F$ and $y \cdot G(y)$.

From the slope of each line (Fig. 1 and others not shown) valid for a fixed concentration ratio $[M]_o/[P]_o$ a value of $F(\text{obs}) = y \cdot F$ is obtained. In Fig. 2a these points are plotted for the three NaCl concentrations applied. We see that the F curves exhibit the same shape and dependence on the ionic strength as reported earlier [1] for the conventional titration curves with Tb^{3+}. However, the F(obs) values now represent the average contact contribution from a set of selected Ln^{3+}, and not the total shift δ_j^{para} from a single ion as in Ref. 1.

Calculations of the F(obs) and G(obs) values from the experiments mentioned above showed that Eu^{3+} gave an almost pure contact shift. Hence, the ratio between the total paramagnetic shift and the contact shift, i.e. $y \cdot \delta_{Eu}^{para}/y \cdot F \cdot \langle S_z \rangle_j$, was 1.06 in 0.1 M NaCl at $[M]_o/[P]_o = 0.1$ for Eu^{3+}. This justified the use of this particular ion alone in some experiments. Here the four other ions (La^{3+}, Tb^{3+}, Ce^{3+} and Pr^{3+}) were employed together with Eu^{3+} at one single Ln^{3+} concentration. This made it possible to calculate $y \cdot \delta_{Eu}^{para}/y \cdot F \cdot \langle S_z \rangle_j$ in order to check that no drastic conformational changes had occurred which would make comparisons between experiments difficult.

The observed enhanced Ln^{3+}-induced shifts in the presence of NaBr and $NaNO_3$ compared to NaCl at the same concentrations are seen in Fig. 2a–c where the experimental F(obs) values as functions of $[M]_o/[P]_o$ are shown for different concentrations of these salts. With $NaNO_3$ as electrolyte the stability of the vesicles in the presence of Ln^{3+} seems lower than in the other two salts.

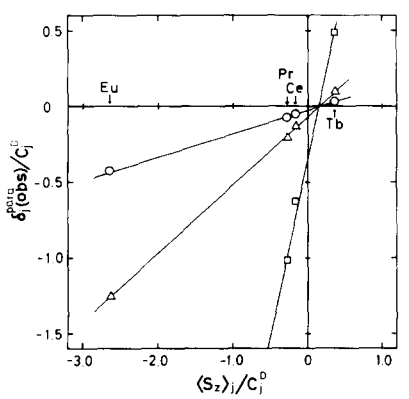

Fig. 1. Plot according to Eqn. 3 of the ^{31}P chemical shifts, δ_j^{para}(obs), for various Ln^{3+} at three different values of the molar ratio $[M]_o/[P]_o$ (○, $4.9 \cdot 10^{-3}$; △, $1.45 \cdot 10^{-2}$, and □, $8.21 \cdot 10^{-2}$). The total lipid concentration was 62.2 mM, corresponding to $[P]_o = 40.4$ mM from the outer bilayer. 0.5 M NaCl in ^2H_2O, pH about 4 (meter reading). Temperature 30°C.

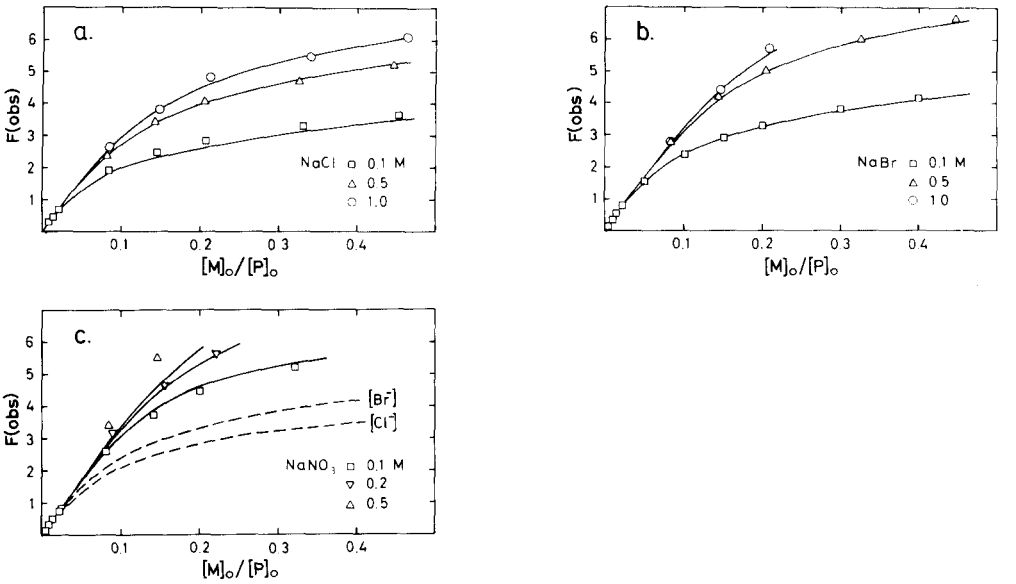

Fig. 2. The experimental contact contributions, $F(\text{obs}) = y \cdot F$, derived from graphs of the kind demonstrated in Fig. 1. The titration curves have been measured at different concentrations of three sodium salts. ———, theoretical curves simulated with the parameters presented in Table II. The total lipid concentration was in all cases close to 60 mM. (a) NaCl; (b) NaBr; (c) $NaNO_3$. The experimental titration curves (- - - - - -) for 0.1 M NaCl and NaBr (from (a) and (b)) are also included. The fraction of phospholipids bound (y) can be calculated from the curves with $y = F(\text{obs})/F$, where $F = 17$.

The vesicles started to aggregate, as noted from the increased turbidity, in 0.5 M $NaNO_3$ already at quite low values of $[M]_o/[P]_o$ and this is probably the reason why we fail to simulate the experiment at this concentration. The NMR signals in $NaNO_3$ are also broader than in the other two salts which makes the evaluation of the shifts less accurate. In Fig. 2c we have for comparison included the experimental curves (broken lines) for the other two sodium salts at 0.1 M.

Some examples of the F curves at very low Ln^{3+} concentrations are shown in

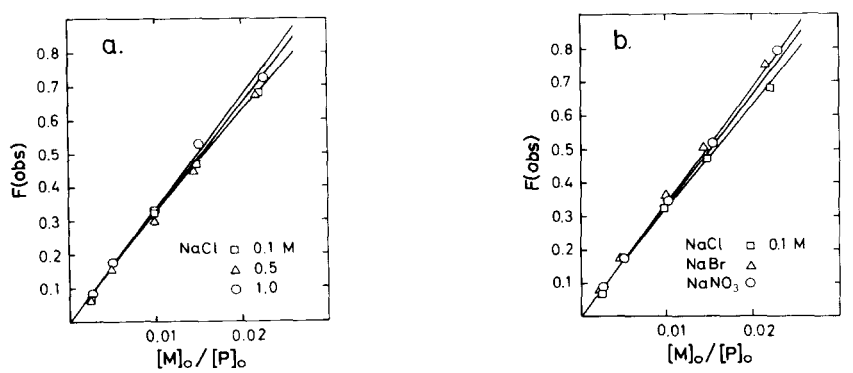

Fig. 3. (a) The expanded initial parts of the same curves as found in Fig. 2a. ———, simulated with the parameters in Table II. (b) The expanded initial parts for the titration curves in Figs. 2a—c for 0.1 M sodium salts with different anions. Total lipid concentration close to 60 mM. ———, simulated with the parameters in Table II.

Fig. 3a and b. For $[M]_o/[P]_o < 0.02$ the shifts are quite insensitive to the total salt concentration (Fig. 3a) and the effect of the anion nature is still small (Fig. 3b). All the nine experiments (including La^{3+}, Ce^{3+}, Eu^{3+} and Tb^{3+}) in Fig. 2 also covered the small Ln^{3+} concentrations employed in Fig. 3. In all cases the same dependence on the electrolytes as seen in Fig. 3 was noticed. Obviously the specific anion effects are most easily seen at fairly high Ln^{3+} concentrations ($[M]_o/[P]_o > 0.1$) and the shift enhancement follows the order $Cl^- < Br^- < NO_3^-$.

From the graphs of the type illustrated in Fig. 1 it is possible to extract F(obs) from the slopes and G(obs) from the intercepts (cf. Eqn. 3). For all nine titration curves included in Fig. 2a—c the corresponding values of $F/G(y) = F(\text{obs})/G(\text{obs})$ values have been calculated. As an example the results from experiments with vesicles in NaCl solutions are presented in Fig. 4. In spite of the scattering of the points, due to difficulties to determine F(obs) and G(obs) with high precision, the three sets of experiments with NaCl (Fig. 4) and the corresponding ones with NaBr and $NaNO_3$ (not shown) all reveal the same tendency of a decrease of $F/G(y)$ in the beginning of the curves.

We have repeated the initial slope experiments using Eu^{3+} instead of Tb^{3+} employed earlier [1]. In Fig. 5 the experimental points with vesicles in 0.1 M NaCl, NaBr and $NaNO_3$ are plotted according to Eqn. 10.

In order to minimize the effects of the anions we also carried out experiments with vesicles prepared in salt-free solution. Only Eu^{3+} has been used in this case and the titrations were done in two different ways. In the conventional way concentrated solutions of $EuCl_3$ or $Eu(NO_3)_3$ were added to vesicle solutions (60 mM phosphatidylcholine in ^2H_2O). In this way the electrolyte concentration can be kept low but will steadily increase. The titration curves do not exhibit any saturation tendency. For $[Eu]_o/[P]_o > 0.01$ it was obvious that the shift produced by the addition of $Eu(NO_3)_3$ was larger than for $EuCl_3$. An alternative way to do the titrations is shown in Figs. 6 and 7, where a concentrated salt-free vesicle solution has been added to dilute Eu^{3+} solutions. In

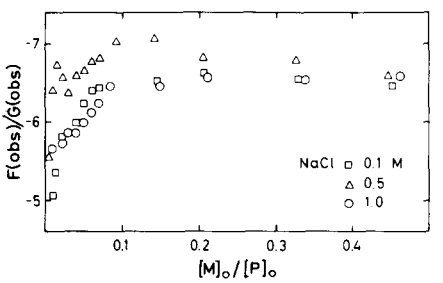

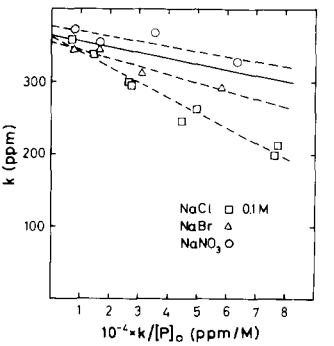

Fig. 4. Plot of the ratio between the contact, F(obs), and the pseudo-contact, G(obs), contributions to the paramagnetic shift (cf. Eqn. 2) for varying Ln^{3+} loading and at different NaCl concentrations. The corresponding F curves are found in Fig. 2.

Fig. 5. The initial slope values (k) for ordinary titration curves plotted according to Eqn. 10. Vesicle solutions with varying lipid concentrations ($[P]_o$: 2.6—43.9 mM) were titrated with $EuCl_3$ in the presence of 0.1 M NaCl, NaBr and $NaNO_3$. ———, calculated with the parameters in Table II for the NaCl case.

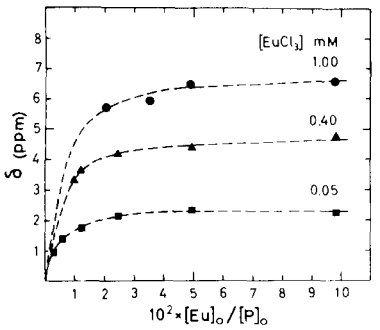

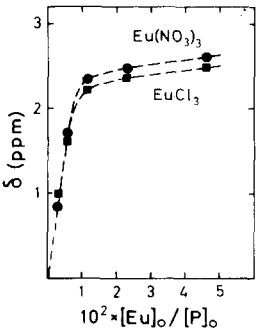

Fig. 6. Titration of $EuCl_3$ solutions with phosphatidylcholine vesicles prepared in salt-free solution (^2H_2O adjusted to pH about 4). The induced chemical shifts (ppm) are the directly measured values.

Fig. 7. Titration of 0.1 mM $EuCl_3$ and $Eu(NO_3)_3$ solutions with phosphatidylcholine vesicles prepared in salt-free solution (^2H_2O adjusted to pH about 4).

this way the ionic strength is kept constant and as seen in Fig. 6 this will produce titration curves which show saturation behaviour. Fig. 7 demonstrates that also with this titration procedure the nitrate gives larger shifts than the chloride. The ratio of the total observed paramagnetic shift to the contact part (vide supra) for Eu^{3+} was calculated at one concentration of Ln^{3+} and found to be 1.066 showing that Eu^{3+} still gives an almost pure contact shift making comparisons with the earlier experiments in salt solutions meaningful.

For the Ln^{3+} complexes with phosphatidylcholine vesicles the binding is influenced by potential effects and all these experiments (Figs. 2a—c and 3a and b) have to be simulated by solving the system of equations mentioned before. For values of K_{MX} in Eqn. 4 we are referred to literature values, which unfortunately differ quite a lot between the various investigators. We have selected the values in Table II as being the most reliable. These values are valid at an ionic strength of 1 M.

TABLE II

PARAMETERS USED FOR THE SIMULATIONS OF THE LANTHANIDE-INDUCED CHEMICAL SHIFT CURVES WITH PHOSPHATIDYLCHOLINE VESICLES (FIGS. 2 AND 3)

Anion X^-	[NaX] (mol/l)	$\gamma_X = \gamma^{\pm}_{NaX}$ [a]	$\gamma_M = \gamma^{\pm}_{MX_3}$ [b]	K_{MX} (l/mol) [c]	K_n^* (l/mol)	K_X (l/mol)	n	F
Cl^-	0.1	0.77	0.49					
	0.5	0.68	0.34	0.9	700	0.9	2	17
	1.0	0.66	0.30					
Br^-	0.1	0.78	0.49					
	0.5	0.69	0.34	0.65	700	2.0	2	17
	1.0	0.69	0.30					
NO_3^-	0.1	0.76	0.39					
	0.2	0.71	0.31	1.4	700	8.0	2	17
	0.5	0.62	0.21					

[a] From Ref. 23.
[b] From Refs. 20—22.
[c] From Refs. 17—19; values refer to an ionic strength of 1 M.

For γ_{MX} we lack information and have to assume that $\gamma_{MX} = \gamma_M$. Mean ion activity factors [20—23] for the pure salts at the same ionic strength as in the actual experiment have been used instead of single ion activity factors which are not available in the literature.

A reasonably good fit to the experimental curves in Figs. 2 and 3 (full lines) was obtained by the set of parameters given in Table II. For the initial slope experiment in Fig. 5 we determined $n \cdot \delta_j^{para} = -364$ ppm as a mean value for Eu^{3+}. If we approximate the induced shift from this particular ion as being a pure contact shift we get from Eqn. 2, $n \cdot F = n \cdot \delta_j^{para}/\langle S_z \rangle_j = 34.0$. This value was used for the simulations. Simulation of the initial slope experiment with the parameters in Table II used in Eqn. 10 resulted in lines with slopes deviating from those given by the experimental points (Fig. 5).

Simulations of the titration experiments carried out at very low ionic strength (Figs. 6 and 7) resulted in too low shifts compared to the experiment with the parameters from Table II.

We have also undertaken a ^{31}P NMR study of L-α-glycerophosphorylcholine as a model compound. In this case one does not have any surface phenomena governed by the electrolyte concentration. Glycerophosphorylcholine in distilled water as well as 0.1 M NaCl has been titrated with various Ln^{3+}. As expected, the induced shifts with this compound were insensitive to the presence of NaCl. The initial slope experiment will in this case allow an immediate determination of the binding constant since no potential effects are involved ($\psi = 0$). Experiments with varying concentrations of glycerophosphorylcholine titrated with $EuCl_3$ (0.1 M NaCl) when plotted according to Eqn. 10 furnished a straight line. From the slope $K_n^* = 2.9$ l/mol and from the intercept $n \cdot \delta_j^{para} = -303$ ppm were obtained. Assuming a 1 : 1 stoichiometry for the complex we get $\delta_j^{para} = -303$ ppm. Also in this case the ratio of total paramagnetic shift to contact shift for Eu^{3+} was checked by using the four other Ln^{3+} together with Eu^{3+} at one single Ln^{3+} concentration. This ratio was calculated to be 1.048.

Discussion

We have designed the experiments to be able to calculate the so-called F curves which give expressions of the contact shifts and should therefore reflect the real binding curve for an average Ln^{3+}. Working with the F curves makes us confident that the shape of the curves, the effects of ionic strength and the specific anion used are not merely a result of conformational changes of the phosphate moieties, which might affect the balance between the contact and the pseudo-contact contributions to the shifts.

From the variation of the $F(obs)/G(obs) = F/G(y)$ values as a function of Ln^{3+} addition (Fig. 4) we have some evidence that a conformational change might take place upon ion binding. Due to the tedious task to produce $F/G(y)$ curves we restricted ourselves to only three paramagnetic Ln^{3+}. However, for the points at 0.5 M NaCl in Fig. 4 the number of ions was four. It is not possible to give a good estimate of the errors (including systematic ones) in the $F/G(y)$ values. From their ^{31}P NMR study, Brown and Seelig [8] noticed a change in the chemical shift anisotropy in the presence of relatively high con-

centrations of Ln^{3+}. Our results suggest a possible conformational change completed at low Ln^{3+} concentrations.

In the present work we have attempted to simulate the complete F curves, from very low to high ion binding. Hence, the parameters in Table II are those selected to give as good as possible overall fit to the experiments. We then had to use a higher chloride binding constant than reported earlier [1]. This also resulted in an F parameter, which agreed well with the initial slope experiment. The parameters used for the simulations of the F curves do, however, not give the right slope in the simulations of the initial slope curves. One possible explanation could be that the Eu^{3+} adsorb to the walls of the NMR tubes, thereby lowering the effective bulk concentration. This would be especially noticeable at the lowest Eu^{3+} concentrations used (i.e. at low $[P]_o$ values). The two control experiments performed showed that this explanation is probably not true. In the initial slope experiment (Fig. 5) the total anion concentration was 0.1 M, but $[P]_o$ varied between 2.6 and 43.9 M. The experiments with the full F curves were carried out only at one lipid concentration, close to the higher value. If our description of the anion binding mechanism is too primitive (vide infra) we expect problems when trying to simulate the experiments at all $[P]_o$ values with the same set of parameters. However, the initial slope curves can be simulated satisfactorily with the same relative ratio between the three K_X values as used for the F curves (Table II), but then lower absolute values must be employed (K_X = 0.2 l/mol for Cl^-). These lower values are, however, too low to give good simulations of the full F curves (Figs. 2 and 3).

Earlier [1] we found large discrepancies between the so-called limiting shift values. Our new extensive results support that a stoichiometry factor $n = 2$ is valid for the lanthanide-phosphatidylcholine complex. In our earlier study we had selected $n = 3$, but also indicated the ambiguity about the stoichiometry. For simplicity we have assumed a single well-defined complex to exist neglecting any possible effects of cooperativity in the surface. Hauser et al. [3,4] using a Langmuir isotherm have suggested that $n = 2$, but as their studies were not based on a thorough analysis of the potential effects a direct comparison is difficult. The stoichiometry used by others [3–7] in a Langmuir isotherm treatment is not directly comparable to our n value when $n \neq 1$ [1].

The values in Table II should be regarded as representative and not unique due to the complex system requiring many parameters for the simulations. Moreover, there are uncertainties in literature values for the K_{MX} constants and the activity coefficients. The reason to introduce activities was to account for the large variation in the ionic strength within our experiments.

From the initial slope experiment with L-glycerophosphorylcholine we noticed that its binding constant to Eu^{3+} is much lower than for phosphatidylcholine vesicles. However, the values for $n \cdot F$ almost agree (28.4 and 34.0, respectively). Our binding constant for the glycerophosphorylcholine complex (2.9 l/mol) is not too far from the value reported by Hauser et al. [9], who however measured in the presence of Cd^{2+} and at a higher pH value. For the Co^{2+} complex, McLaughlin et al. [24] have determined the binding constant to be 0.2 l/mol. (Notice that they in the summary by mistake refer to the binding constant as 5.1 mol/l.)

Accounting for the influence of anions in case of the phosphatidylcholine

membrane is very crucial for the simulations. We have made attempts to simulate the experiments without any direct anion binding to the surface. Attempts to simulate binding of LnX^{2+} alone or in parallel with Ln^{3+} were not successful. Also the experiment in salt-free medium (Fig. 7) indicates that binding of LnX^{2+} alone can be ruled out since the difference between $EuCl_3$ and $Eu(NO_3)_3$ would have been greater. Although we feel that the ratio between the anion binding constants K_X has been correctly established (Cl^- : Br^- : NO_3^-; 1.0 : 2.2 : 8.8) we would prefer to consider them as phenomenological parameters for the phosphatidylcholine-Ln^{3+} system.

Indications of specific anion effects also come from proton NMR [25] and Raman [26] studies of phosphatidylcholines. The electrophoretic mobility of phosphatidylcholine liposomes in various monovalent potassium salts has been studied by Barsukov et al. [13]. They report the mobility to be 3.1 times higher in nitrate medium compared to chloride. (However, from Table III in Ref. 13 we understand that this factor should be 9.7.) The mobility for liposomes in 0.15 M KCl was reported to be $-0.15 \pm 0.01\ \mu m \cdot s^{-1} \cdot cm \cdot V^{-1}$. This low mobility should correspond at maximum to a few mV ζ-potential according to the Helmholtz-Smoluchowski formula. The surface potential in 0.15 M KCl, in the absence of Ln^{3+}, may be estimated from our theoretical approach if we assume the K^+ adsorption to be negligible. With $K_X = 0.91$ l/mol for Cl^- this potential will become too negative compared to the ζ-potential mentioned. Barsukov et al. [13] reported binding constants for the Cl^- and NO_3^- adsorption to phosphatidylcholine (1.67 and 4.03 l/mol, respectively). They followed the ^{31}P NMR shift from Pr^{3+} and applied a Langmuir isotherm without discussing the potential effects. If the binding constants given [13] really are intrinsic parameters, and not apparent, a discrepancy with the electrophoretic results obviously exists.

McLaughlin et al. [5] claim that they do not need to introduce any specific Cl^- binding to vesicles in their ^{31}P NMR study of the Co^{2+} interaction. They also measured the ζ-potential for various Ca^{2+} concentrations. From their diagram (Ref. 5, page 347, Fig. 2) one can imagine a small negative potential to exist in the absence of Ca^{2+}, indicating a weak Cl^- binding to phosphatidylcholine (notice the logarithimic discontinuous concentration scales). We can simulate the experiments by McLaughlin et al. quite well, with the binding constants reported earlier by us [1]. There we used a weak Cl^- binding (K_X = 0.065 l/mol).

Trusting the electrokinetic studies [5,13] we like to suggest that the specific adsorption of Cl^- to the phosphatidylcholine membrane is weak in the absence of adsorbed cations and that the anion binding is enhanced in the presence of adsorbing cations. Hence, different K_X values would apply to vesicles with Ca^{2+} and Ln^{3+}. We have therefore considered the following surface reactions with anions:

$$X^- + P \rightleftharpoons XP^-$$
$$X^- + LnP_2^{3+} \rightleftharpoons XLnP_2^{2+}$$
$$X^- + CaP^{2+} \rightleftharpoons XCaP^+$$

It is quite reasonable to assume that this mechanism would lead to stronger anion binding in the presence of Ln^{3+} compared to Ca^{2+}. One further binding

constant is required, increasing the complexity considerably. We refrain from further calculations since we feel that a discrete-charge treatment is most relevant for this model for anion binding. This is a difficult task since the charge distribution is not constant during a titration. Further investigations will be necessary to settle the problem of cation-specific adsorption of anions to the phosphatidylcholine membrane.

The Gouy-Chapman theory has proved to be surprisingly successful considering all the inherent assumptions. The large variation in ionic strength (0—1.0 M) means that the Debye length is changing considerably. For 1 M NaCl this length must be small (order of Å). We have therefore considered to apply a discrete-charge model in our investigation. The most simple form of such a theory is based on the linearized form of the Debye-Hückel theory [27]. Our system of equations is too complicated to be handled in this simple form. A more complete treatment of the discrete-charge theory, in a form more relevant to our problem, does not to our knowledge exist. The greatest need for a discrete-charge model probably exists at the beginning of the titrations, where rather few ions are bound. Then the surface potential is low and $[MP_n]_s << [P]_s$. In Appendix we show with a very simplified treatment how the effective cation binding in this particular case, neglecting anion binding, becomes identical for the discrete-charge and the smeared-charge model. A discrete-charge model where binding of anions parallel with cations takes place would be even more complicated.

Conclusions

We have demonstrated the importance of accounting for surface potential effects upon ion binding to phosphatidylcholine vesicles. Due to the complexity of the problem it has not been possible to determine precise intrinsic binding constants. We have established a specific anion effect. The anion adsorption might depend on the actual metal ion employed since the intrinsic chloride binding constant seems to be larger in the case of the Ln^{3+} than for Ca^{2+}. We have not been able to directly determine the anion adsorption to the phosphatidylcholine vesicles in the absence of interacting cations. An independent measure of anion binding constants would facilitate the interpretation of our results.

In this study we employed Ln^{3+} due to their relative strong intrinsic binding also to neutral lipids and their individual magnetic properties. By using several Ln^{3+} and separate the chemical shifts into contact and pseudo-contact parts we have avoided possible complications from variations of the pseudo-contact part. The results from this procedure demonstrated that the basic properties of the binding curves are intrinsic effects of specific ion binding and potential phenomena. We have some indications that a conformational change takes place already at low ion binding to the surface. The main conclusions from this study should be relevant to the Ca^{2+} interaction with phosphatidylcholine membranes. This ion can be replaced by Ln^{3+} in several biological systems [28].

Appendix

Comparison of the effective ion binding in the case of discrete and smeared charges

The article by Nelson and McQuarrie [27] should be consulted for the theoretical background. We assume the ions with charge z to be uniformly distributed on the phospholipid surface forming a two-dimensional square Bravais lattice with lattice constant a. The potential will then vary in a periodical manner on the surface. We may regard the surface as being divided into squares with the side a and the charge z located at the centre of each area. For each square a coordinate system is defined with origo at the point of the charge. As all squares are identical it is enough to study one such square.

A small amount of ions is added, which can bind to all points on the surface according to:

$$M^z + nP \rightleftarrows MP_n^z$$

Suppose that the ions added are too few to affect the original arrangement of charges. The surface concentration of ions bound at each infinitesimal area $dx \cdot dy$ with origin at the point $(x; y)$, $[MP_n(x, y)]_s$, will depend on the potential at this point, $\psi(x, y)$. We assume that $[MP_n(x, y)]_s << [P(x, y)]_s$, which means that $[P(x, y)]_s \approx [P]_{os}$ for all points.

We then get (cf. Eqn. 6 and the appropriate Boltzmann relation):

$$[MP_n(x, y)]_s = K_n[P(x, y)]_s^n[M]_b \exp(-zF\psi(x, y)/RT)$$

Of interest is the mean concentration over the total surface. We integrate $[MP_n(x, y)]_s$ over the square, and divide by its area

$$[MP_n]_s = \frac{1}{a^2} \int_{-\frac{a}{2}}^{\frac{a}{2}} \int_{-\frac{a}{2}}^{\frac{a}{2}} [MP_n(x, y)]_s \, dx \cdot dy$$

If $\psi << RT/F$ (the condition for the linearized form of the Debye-Hückel theory)

$$[MP_n]_s = \frac{1}{a^2} \iint K_n[M]_b[P]_{os}^n (1 - zF\psi(x, y)/RT) \, dx \cdot dy$$

Applying the potential derived in Ref. 27 (Eqn. 29) this integral can be evaluated. The result is

$$[MP_n]_s = K_n[M]_b[P]_{os}^n (1 - zF\psi/RT)$$

where ψ now is the potential for the smeared-charge case (Ref. 27, Eqn. 25).

With $\psi << RT/F$ and $[P]_s \approx [P]_{os}$, which is true if $[P(x, y)]_s \approx [P]_{os}$, we get:

$$[MP_n]_s = K_n[M]_b[P]_s^n \exp(-zF\psi/RT)$$

which is the form of the equation used in the present study (Eqn. 6 combined with the appropriate Boltzmann relation).

Acknowledgements

We like to thank Prof. Anders Ehrenberg for his continuous interest in this work and for the facilities placed at our disposal. The skilful technical assistance by Mrs. Karin Rydström and Miss Maria Dalin was much appreciated. Dr. Hans Grasdalen, the University of Trondheim, and Dr. Bo Cartling contributed with valuable discussions. This study was supported by the Swedish Natural Science and Medical Research Councils as well as the Knut and Alice Wallenberg Foundation and the Magn. Bergvall Foundation.

References

1 Grasdalen, H., Eriksson, L.E.G., Westman, J. and Ehrenberg, A. (1977) Biochim. Biophys. Acta 469, 151–162
2 Hutton, W.C., Yeagle, P.L. and Martin, R.B. (1977) Chem. Phys. Lipids 19, 255–265
3 Hauser, H., Phillips, M.C., Levine, B.A. and Williams, R.J.P. (1975) Eur. J. Biochem. 58, 133–144
4 Hauser, H., Hinckley, C.C., Krebs, J., Levine, B.A., Phillips, M.C. and Williams, R.J.P. (1977) Biochim. Biophys. Acta 468, 364–377
5 McLaughlin, A., Grathwohl, C. and McLaughlin, S. (1978) Biochim. Biophys. Acta 513, 338–357
6 Puskin, J.S. (1977) J. Membrane Biol. 35, 39–55
7 Nir, S., Newton, C. and Papahadjopoulos, D. (1978) Bioelectrochem. Bioenerg. 5, 116–133
8 Brown, M.F. and Seelig, J. (1977) Nature 269, 721–723
9 Hauser, H., Guyer, W., Levine, B., Skrabal, P. and Williams, R.J.P. (1978) Biochim. Biophys. Acta 508, 450–463
10 Barsukov, L.I., Shapiro, Yu.E., Viktorov, A.V., Volkova, V.I., Bystrov, V.F. and Bergelson, L.D. (1976) Bioorg. Khim. 2, 1404–1415
11 Reilley, C.N., Good, B.W. and Desreux, J.F. (1975) Anal. Chem. 47, 2110–2116
12 Reilley, C.N., Good, B.W. and Allendoerfer, R.D. (1976) Anal. Chem. 48, 1446–1458
13 Barsukov, L.I., Volkova, V.I., Shapiro, Yu.E., Vikotorov, A.V., Bystrov, V.F. and Bergelson, L.D. (1977) Bioorg. Khim. 3, 1355–1361
14 Fiske, C.H. and Subbarow, Y. (1925) J. Biol. Chem. 66, 375–386
15 Rinehart, R.W. (1954) Anal. Chem. 26, 1820–1822
16 Hopper, M.J. (1973) Harwell Subroutine Library, A Catalogue of Subroutines, Theor. Phys. Div., A.E.R.E., Harwell
17 Peppard, D.F., Mason, G.W. and Hucher, I. (1962) J. Inorg. Nucl. Chem. 24, 881–888
18 Choppin, G.R. and Unrein, P.J. (1963) J. Inorg. Nucl. Chem. 25, 387–393
19 Bansal, B.M.L., Patil, S.K. and Sharma, H.D. (1964) J. Inorg. Nucl. Chem. 26, 993–1000
20 Spedding, F.H., Nelson, R.A. and Rard, J.A. (1974) J. Chem. Eng. Data 19, 379–381
21 Spedding, F.H., Weber, H.O., Saeger, V.W., Petheram, H.P., Rard, J.A. and Habenschuss, A. (1976) J. Chem. Eng. Data 21, 341–360
22 O'Brien, W.G. (1974) Dissertation Iowa State University, Report 1974, IS-T-621, Dep NTIS
23 Robinson, R.A. and Stokes, R.H. (1949) Trans. Faraday Soc. 45, 612–624
24 McLaughlin, A.C., Grathwohl, C. and Richards, R.E. (1978) J. Magn. Res. 31, 283–293
25 Jendrasiak, G.L. (1972) Chem. Phys. Lipids 9, 133–146
26 Loshchilova, E. and Karvaly, B. (1978) Biochim. Biophys. Acta 514, 274–285
27 Nelson, A.P. and McQuarrie, D.A. (1975) J. Theor. Biol. 55, 13–27
28 Switzer, M.E. (1978) Sci. Prog. Oxf. 65, 19–30